Computational Materials Science 69 (2013) 304–310

Contents lists available at SciVerse ScienceDirect

Computational Materials Science

journal homepage: www.elsevier.com/locate/commatsci

Young's modulus estimation based on high symmetry 3-D finite element model for metal matrix composites

I. Alfonso [a,*], I.A. Figueroa [b], J.M. Sierra [a], M. Abatal [a], G. Gonzalez [b], V. Rodriguez-Iglesias [a], A. Medina-Flores [c], J.E. Flores [a]

[a] Facultad de Ingeniería, Universidad Autónoma del Carmen, Campus III, Avenida Central S/N, Esq. con Fracc. Mundo Maya, C.P. 24115, Ciudad del Carmen, Campeche, Mexico
[b] Instituto de Investigaciones en Materiales, Universidad Nacional Autónoma de Mexico, Circuito Exterior SN, Ciudad Universitaria, C.P. 04510, Del. Coyoacán, México, DF, Mexico
[c] Instituto de Investigaciones Metalúrgicas, Universidad Michoacana de San Nicolás de Hidalgo, Edificio U. Ciudad Universitaria, C.P. 58000, Morelia, Michoacán, Mexico

ARTICLE INFO

Article history:
Received 26 October 2012
Received in revised form 22 November 2012
Accepted 28 November 2012
Available online 8 January 2013

Keywords:
Finite element method
Representative volume element
Unit cell
Composite
Aspect ratio
Elastic modulus

ABSTRACT

The Young's moduli of Al356/SiC (particle) Metal Matrix Composite (MMC) with different particle aspect ratios were estimated by Finite Elements Analysis (FEA), using a simple 3-D model. The results were compared to a 2-D axisymmetric FEA model, to the experimental results, and the predicted values obtained from the Rule of Mixtures and the Halpin–Tsai (HT) model. FEA software ANSYS 11.0 was used. The 3-D model consisted on taking the one-eight part of a unit cell, with particles having cylindrical shape, a volume fraction of 0.12 and aspect ratio from 0.2 to 1.8. The estimated Young's moduli presented significant differences, mainly at aspect ratios higher than 1.0, resulting the 3-D model estimations closer to the experimental values. The results from the selected 3-D model were found to have higher accuracy when compared to traditional axisymmetric 2-D model. Besides, the efficiency of this high symmetry 3-D model showed that a more complex 3-D model is not necessary.

1. Introduction

Metal matrix composites, and mainly aluminum matrix composites, are materials that have been successfully used for many applications, this is due to their attractive lightweight and superior mechanical and thermal properties [1–3]. Particle reinforced MMCs are also rather attractive since their almost isotropic properties, ease of fabrication, and low cost. Tensile strength, elastic modulus and high temperature stability of MMCs are higher than those of monolithic alloys, while their ductility, fatigue and fracture toughness properties are considerably lower [4]. These properties depend on the particles volume fraction, distribution, aspect ratio, size, orientation and interfacial bonding [1]. There are numerous analytical and numerical models for the prediction of mechanical behavior of composite materials, with reasonably low errors [5–7]. The analytical models mainly include the Eshelby model, the self-consistent model, the variational principles of elasticity theory, the composite cylinder model and other unit-cell models [8–11]. These models normally involve simplified assumptions and a uniform Representative Volume Element (RVE) or unit-cell, which captures the major features of the microstructure. Numerical methods usually contain less simplifying assumptions both in the mathematical formulation and in the selection of the geometry of the RVE. These methods are also able to provide accurate predictions and mainly include the finite difference method, the finite elements method (FEM or Finite Elements Analysis, FEA), and the boundary element method [8–11]. An easy way to evaluate the effective elastic response of a composite with perfect particle–matrix bonding under load, is the conventional Rule of Mixtures. This rule can be formulated for particle-reinforced MMCs as follows [1]:

$$E_c = E_m V_m + E_p V_p, \tag{1}$$

where E and V are respectively the Young's modulus and volume fraction, for the matrix (m) and the particles (p). As observed, the volume fraction of particles in a MMC plays a determining role, affecting the elastic properties. Nevertheless this model does not take into account the particle aspect-ratio. A simple Rule of Mixtures approach is inexact when estimating the effective modulus of particle reinforced MMCs. This approach is based on the condition of isostrain between the matrix and the reinforcement, and hence it is more exact for continuous fiber reinforcement with high aspect ratio. That is why others accurate estimations have been made in order to predict anisotropy in Young's modulus: e.g.: the Halpin–Tsai (HT) model, which assumes a perfectly oriented discontinuous reinforcement in the composite, parallel to the applied

* Corresponding author. Tel.: +52 9383811018x1702.
E-mail address: ialfonso@pampano.unacar.mx (I. Alfonso).

0927-0256/$ - see front matter © 2012 Elsevier B.V. All rights reserved.
http://dx.doi.org/10.1016/j.commatsci.2012.11.047

load [12,13]. According to the HT model, the Young's modulus for composites can be determined by:

$$E_c = \frac{E_m(1 + 2sqV_p)}{1 - qV_p}, \quad (2)$$

where E_c, E_p and E_m are respectively the Young's moduli of the composite, the particle and the matrix, s is the aspect ratio of the particle, V_p their volume fraction, and q is a geometrical parameter that can be written as:

$$q = \frac{(E_p/E_m) - 1}{(E_p/E_m) + 2s}, \quad (3)$$

FEA is a viable method to analyze particle dispersed MMCs due to its modeling capability of the particle, being able to model different geometries and analyze their effect on the composite properties [14]. The anisotropy of the reinforcement in composites is challenging, especially when the deformation behavior is modeled, then an adequate selection of the RVE must be done, trying to reproduce the actual morphology, distribution, and orientation of the reinforcing particles. Modeling and simulating MMCs with complicated microstructures is very labor and time consuming. The distribution of the particles within the cross-section of MMCs is likely to be random. It is difficult, if not impossible, to model the composite behavior with the real constituent geometry. Therefore, it is normally assumed that particles are arranged in a regular and periodic square, circular or hexagonal array. Particles and short fibers have been successfully modeled using 2-D and 3-D analysis with different reinforcement shapes: cubic, cylinder, truncated cylinder, double-cone and sphere. The 2-D analysis is impossible to use in many study cases due to the irregularity and the low symmetry of the reinforcement, besides 2-D multi-particle models give results that are quite different from 3-D model ones. The most important 2-D model for these analyses is the axisymmetric case,

Table 1
Aspect ratio, diameter and height for the cylindrical modeled particles.

Aspect ratio (h/d)	Diameter (μm)	Height (μm)
0.2	15.71	3.14
0.6	10.89	6.53
1.0	9.19	9.19
1.4	8.21	11.5
1.8	7.55	13.59

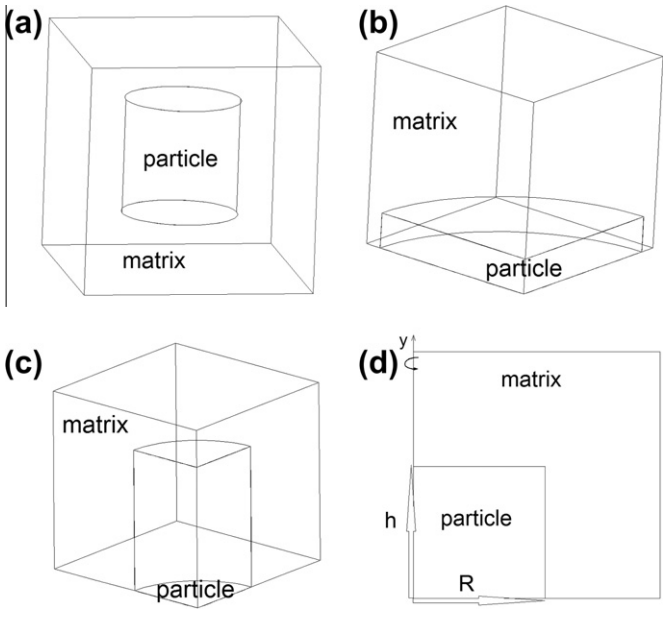

Fig. 1. Cubic periodical unit cell for the particle–matrix system with an aspect ratio of 1.4 (a); RVE with particle aspect ratios of 0.2 (b) and 1.8 (c); and the 2-D axisymmetric model (d).

Table 2
Mechanical properties for Al matrix and SiC particles [1,19].

Material	Young's modulus, E (GPa)	Poisson ratio, v
Aluminum A356 matrix	72.4	0.33
SiC particles	401.4	0.18

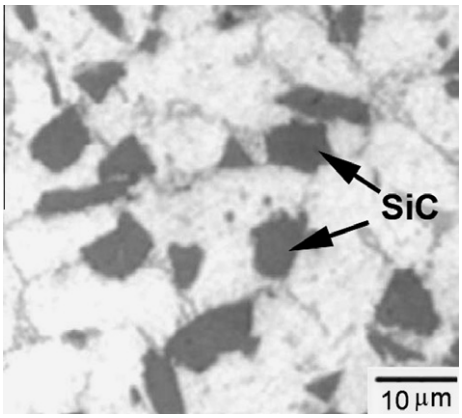

Fig. 2. Optical micrograph of the Al-356/SiC MMC cross-section. Morphology and distribution of the particles can be observed.

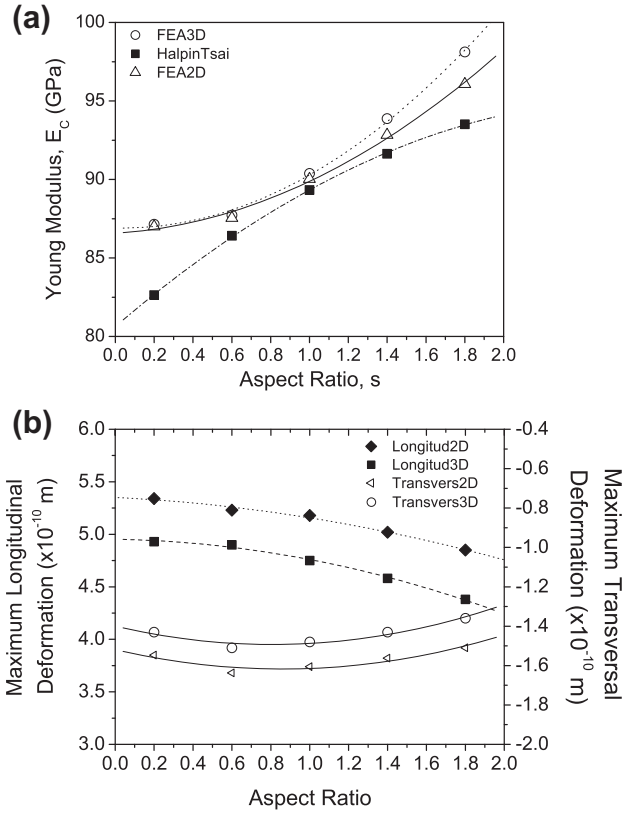

Fig. 3. (a) Variation of Young's moduli estimations for the MMC vs the particles aspect ratio for the studied models. (b) Variation of longitudinal and transversal maximum deformation with aspect ratio.

although the model can be easily transformed in a 3-D analysis case rotating 360° the 2-D model. A 3-D model is necessary in order to predict the material responses such as strain to failure, fracture toughness, and fatigue life, which depend on local events. 3-D models have been used in order to provide a better understanding of the elastic phenomenon and critical zones analysis. Various works have found good relationships between the results obtained by FEA models and the experimental measurements: Kari et al. [15] model used 3-D cubic RVE, composed by various unit-cells, Srikanth et al. [16] used a cylindrical RVE with various particles, while Liu and Chen [17] modeled a composite material using three different RVEs: cylindrical, cubic and hexagonal. Cubic and hexagonal unit cells can idealize the composite in terms of a uniform periodic distribution of the particles in the matrix, exactly matching each unit cell, and describe the morphology of the whole composite. It is also common the use of axisymmetric unit cells (actually cylindrical cell) as an approximation to a three-dimensional hexagonal model. Nevertheless, cylindrical cells cannot be organized in a periodic array without leaving voids or holes. Otherwise, the major inconvenient of hexagonal or cubic 3-D models is the complexity of the unit cell or the RVE, causing an important increase in the computer requirements. That is why the main objective of the present work is to study a simple 3-D model, making special emphasis in obtaining a less complicated RVE, and compare its behavior and geometry with an established 2-D axisymmetric model. In order to achieve this objective, a MMC composed by the alloy Al–7.45Si–0.44Mg reinforced with SiC particles was taken as the starting material. ANSYS 11.0 FEA software was employed for the theoretical calculations, and the results were compared with the experimental values, with the Rule of Mixtures and the HT model.

2. Experimental and calculation

A MMC comprising Al–7.45Si–0.44Mg alloy, reinforced with SiC particles, was obtained as 2 mm diameter wires using the Ohno Continuous Casting (OCC) method. This process consists on a mold heated at a temperature few degrees higher than the solidification temperature of the molten metal. By controlling the solidification mechanism, it is possible to reduce the friction and produce small diameter wires (2 mm), including particle reinforced MMCs [18]. Cross-sections of the obtained MMC were polished with standard metallographic techniques and examined by optical microscopy. Sigma Scan Pro 5.0 software was used to determine the volume fraction, average size and aspect ratio of the reinforcement SiC particles. The obtained data were used as base conditions for modeling the MMC with ANSYS 11.0, and are as follow: the SiC particles presented irregular shapes, their minimum and maximum average lengths were 6.31 ± 3.75 μm and 14.72 ± 4.24 μm, respectively; the volume fraction and average aspect ratio were 0.12 ± 0.02 and 1.40 ± 0.49, respectively. In order to generate these features and analyze the effect of the aspect ratio on the Young's modulus, homogeneous distribution of the particles was assumed and different dimensions and aspect ratio of the particles were used, as shown in Table 1. Note that the height and diameter values are dependent of the aspect ratio and volume of the particles. The vol-

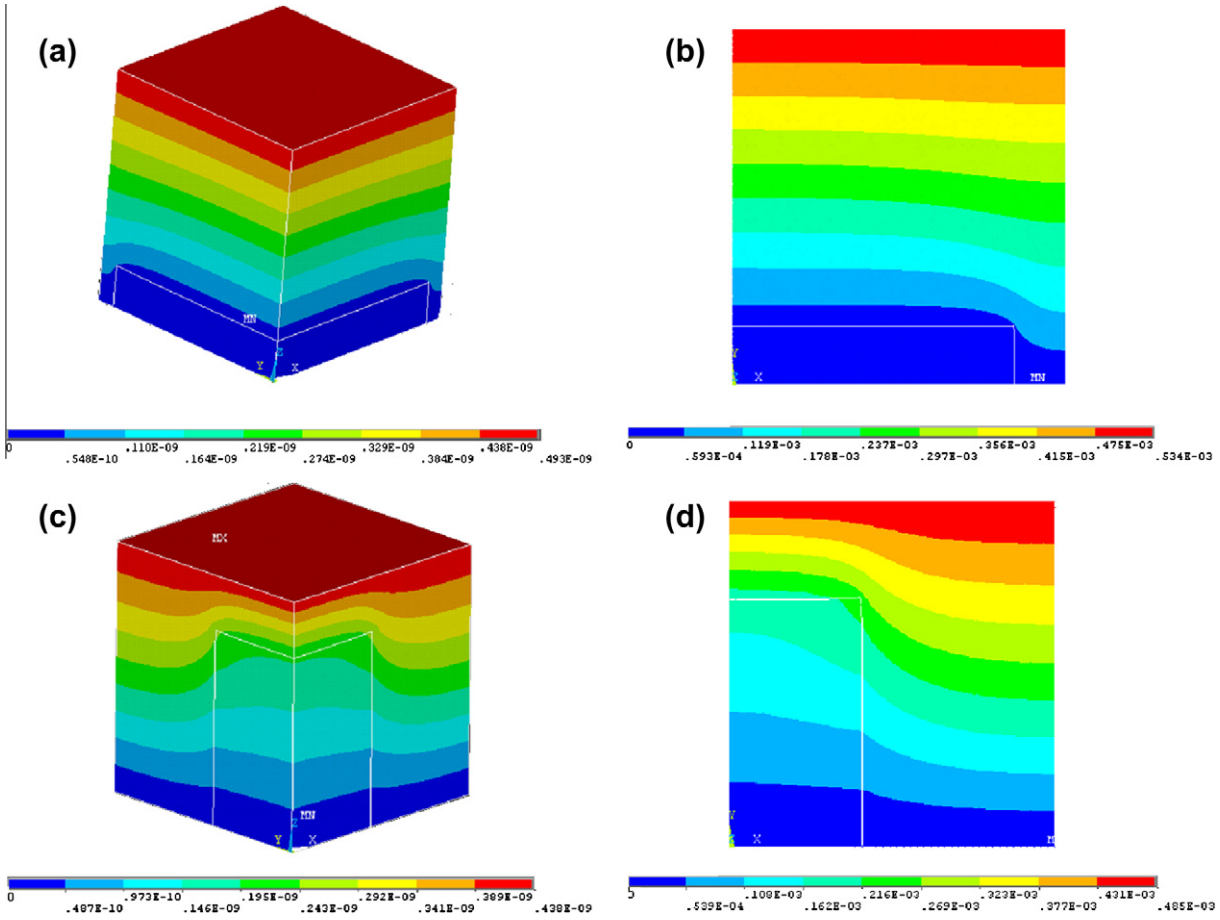

Fig. 4. Deformation of the RVEs under uniaxial load for the MMC reinforced with particles: (a) aspect ratio of 0.2 using a 3-D RVE, (b) aspect ratio of 0.2 using an axisymmetric 2-D model, (c) aspect ratio of 1.8 using a 3-D RVE, and (d) aspect ratio of 1.8 using an axisymmetric 2-D model.

ume fraction and volume of the particles remained constant: for the 3-D simulation, the particles were modeled as cylinders of 610 μm^3, whilst the matrix that surrounds the cylindrical particle was considered as a cube of 5080 μm^3.

The obtained unit-cell is shown in Fig. 1a, where $a = b = 17.19$ μm. This cell represents the particle–matrix system, and their repetition in the space reproduces the MMC. As mentioned above, the RVE consists on one-eight symmetric part of the unit-cell. This RVE allows a better analysis of stress distributions. Fig. 1b and c show the RVE for the model of particles with aspect ratios of 0.2 and 1.8, respectively. For the axisymmetric model, the RVE is cylindrical, obtained from the revolution of the square around *Y* axis (Fig. 1d). In this figure a cylinder with a radius *R* and height *h* is represented. The left vertical boundary (*Y* axis) represents the axially symmetric axis, while mirror symmetry exists about the bottom boundary (*X* axis). The aspect ratios and particles volume fraction were the same for the axisymmetric and 3-D models.

The properties of the material used for the analysis are given in Table 2. The experimental Young's modulus for the wires obtained by the OCC process was determined using a GrindoSonic Mk5, following ASTM E1876-97, and will be further compared to the estimated values for validation purposes.

For the 3-D model, a 10-nodes high order 3-D solid element (Solid187) was selected to create the finite element mesh. This element has a quadratic displacement behavior and is well suited for modeling irregular meshes. Each of the 10 nodes has three degrees of freedom: translations in the nodal *X*, *Y*, and *Z* directions. The nodes of the bottom were fully constrained (zero displacement), while nodes of the *YZ* and *XZ* planes were constrained in *X* and *Y* directions, respectively, using the coupled-node boundary condition (keeping the nodes in the same plane) at faces $X = Lx$, $Y = Ly$, and $Z = Lz$. For the axisymmetric model, 8-Node 2-D Structural Solid (Plane 82) element was used. This element is defined by eight nodes having two degrees of freedom in each node: translations in the nodal *X* and *Y* directions. In this case the coupled-node boundary condition was used for faces *X* (upper) and *Y* (right). This condition is applied since the particles and the matrix have different moduli, provoking un-even surfaces and making the deformation measurement hard to define. It also represents the condition that the composite block is an inclusion in an infinitely large composite, consisting of the same filler particles and matrix [20]. Using both, 3-D and axisymmetric models, Young's moduli of the MMC with different particles aspect ratios were uni-axially estimated when applying a 5 MPa tensile stress on the upper end nodes of the RVE. The stress and strain distributions were also determined.

3. Results and discussion

The optical micrograph in Fig. 2 shows the microstructure of the MMC wires obtained using OCC process. The morphological characteristics of this MMC were used as starting point for FEA estimations in the aforementioned model. The experimental value for the Young's modulus of the wires was 99.67 ± 12.12 GPa, and will be compared with our estimations using the same aspect ratio. The Young's modulus obtained by Rule of Mixtures was 111.88 ± 7.34 GPa. This value remains constant due to the fact that this rule does not take into account the aspect ratio, as shown in Eq. (1).

Fig. 3a shows the comparative behavior of the Young's modulus calculated using the HT model and the FEA models: 3-D proposed in this work and 2-D axisymmetric. The results obtained with the FEA and HT models showed a Young's modulus increment as the aspect ratio increases, resulting FEA values higher than the obtained with the HT model. This behavior could be explained due to the fact that FEA uses a specific morphology for the particles (cylindrical), while HT model does not take into account any specific morphology. It is worth mentioning that although the behavior for both FEA models were very similar for low aspect ratios, the difference in the Young's modulus significantly increases for aspect ratios higher than 1.0, being higher for the 3-D model. In order to analyze this behavior, it is important to remark that for higher aspect ratios, the reinforced role of the particles is higher and the RVE shape becomes critical, this will be further analyzed. The FEA Young's moduli for high aspect ratios was found to be closer to the values of the Rule of Mixture than for low aspect ratios. This could be attributed to the fact that for low aspect ratios, the strengthening effect is low. On the other hand, the Young's modulus predicted by 3-D FEA for the MMC with particle aspect ratio of 1.4 (93.8 GPa) is relatively closer to the experimental result (99.67 ± 12.12 GPa) than the axisymmetric model value (92.1 GPa). It is important to notice that the particle geometry selection leads to a good correlation between aspect ratio and elastic modulus, confirming that the use of more complicated models would be unnecessary. Although the SiC particles in the material contain sharp corners, the experimental values are usually slightly different than the numerical predictions for unit cylinders. This may be attributed to some degree of particle fracture during thermo-mechanical processing, development of residual stresses, and particle clustering in the composite [21].

Maximum longitudinal and transversal deformation behaviors can be observed in Fig. 3b for both, 2-D and 3-D models. The longitudinal deformation decreased while transversal deformation increased for both models in a similar way. The absolute values were higher for the 2-D model. This result showed that the influence of

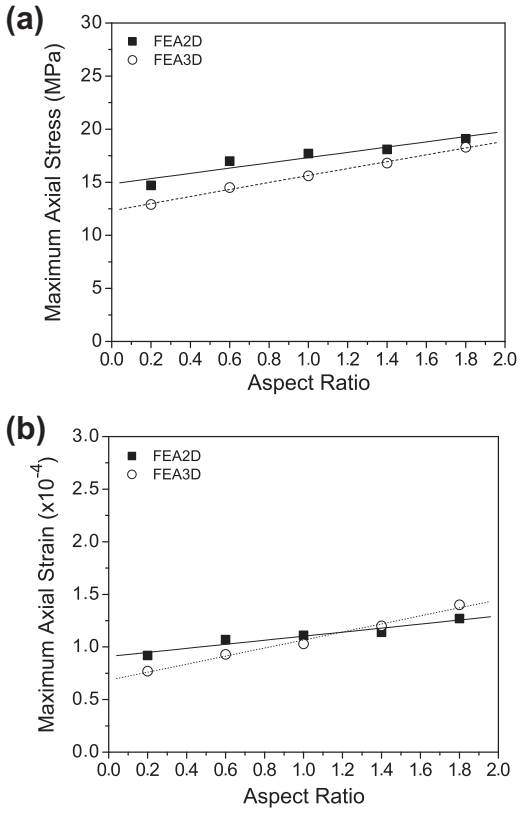

Fig. 5. (a) Effect of the aspect ratio on the maximum axial stress for the 2-D and 3-D models. (b) Effect of the aspect ratio on the maximum axial strains for the 2-D and 3-D models.

the RVE geometry is important: equal particles morphology, aspect ratios, volume and volume fractions tend to generate different results when the RVE shape changes. Our estimations are consistent with the results reported using other FEA models for different composite materials [13,22]. It is also important to mention that the Young's modulus could vary with particle size for a constant volume fraction [23]. The differences between the deformations for the used aspect ratios are less than 10%. This is due to the low aspect ratio of particulate materials, where the load transfer is not as efficient as in the case of continuous fiber reinforcement, but is still significant in providing strengthening. These results are consistent with models and estimations that establish critical reinforcement aspect ratio values, varying with volume fractions. A critical aspect ratio is the required for effective composite performance [24]. For a given reinforcement-matrix combination, the mechanical behavior of the composite also depends on the volume fraction and size of the reinforcement. When the aspect ratio is very large or very small, the composite stresses are almost the same [25].

The graphical response of the RVEs to the distributed applied loads can be observed in Fig. 4a–d for 3-D model (a and c) and for the axisymmetric model (b and d), for aspect ratios of 0.2 and 1.8. As observed, the total deformation is minimum for the SiC particles, which is the material that gives the stiffness and strength to the MMC, and is very similar for both models. This suggests that qualitative deformation responses have not significant differences between 2-D and 3-D models, however, quantitative differences could be critical, as observed in Fig. 3b.

On the other hand, the analysis of the maximum axial stress and strain behavior showed a linear increase with aspect ratio for both 2-D and 3-D models (Fig. 5a and b). As can be observed in Fig. 5a, the maximum stress is higher for the 2-D model than for the 3-D model. Nevertheless this difference decreases for high aspect ratios. In the case of the axial strain, 2-D values are higher for low aspect ratios, although for aspect ratios higher than 1.0 the behavior is opposite, and the values for the 3-D model are higher. This fact could be explained due to the geometry of the RVE, and will be analyzed taking into account the location of the maxima points.

The location of maxima stresses in the particle–matrix interface agrees well with the reported in the literature for microscopy studies, being usually critical points (Fig. 6a–d). The fractures initiate in these points and stress will cause to grow. Particles with higher aspect ratio are under higher stresses, being concentrated at the sharp corners of the particles [26]. For low volume fraction reinforced composites (as in the present case, 0.12), cracks initiate generally at the particle–matrix interfaces [27].

Fig. 7a–d shows the strain distribution for 3-D (Fig. 7a and c) and 2-D model (Fig. 7b and d), for aspect ratios of 0.2 and 1.8. As can be observed, the strain distribution using the two models is similar. For an aspect ratio of 0.2 (Fig. 7a and b) maxima strains are located at the particle–matrix interfaces, while for an aspect ratio of 1.8 (Fig. 7c and d) the maxima are located at the center of the upper side of the RVE. This behavior could be also related to the RVE shape, as for stresses distribution. These figures show that 3-

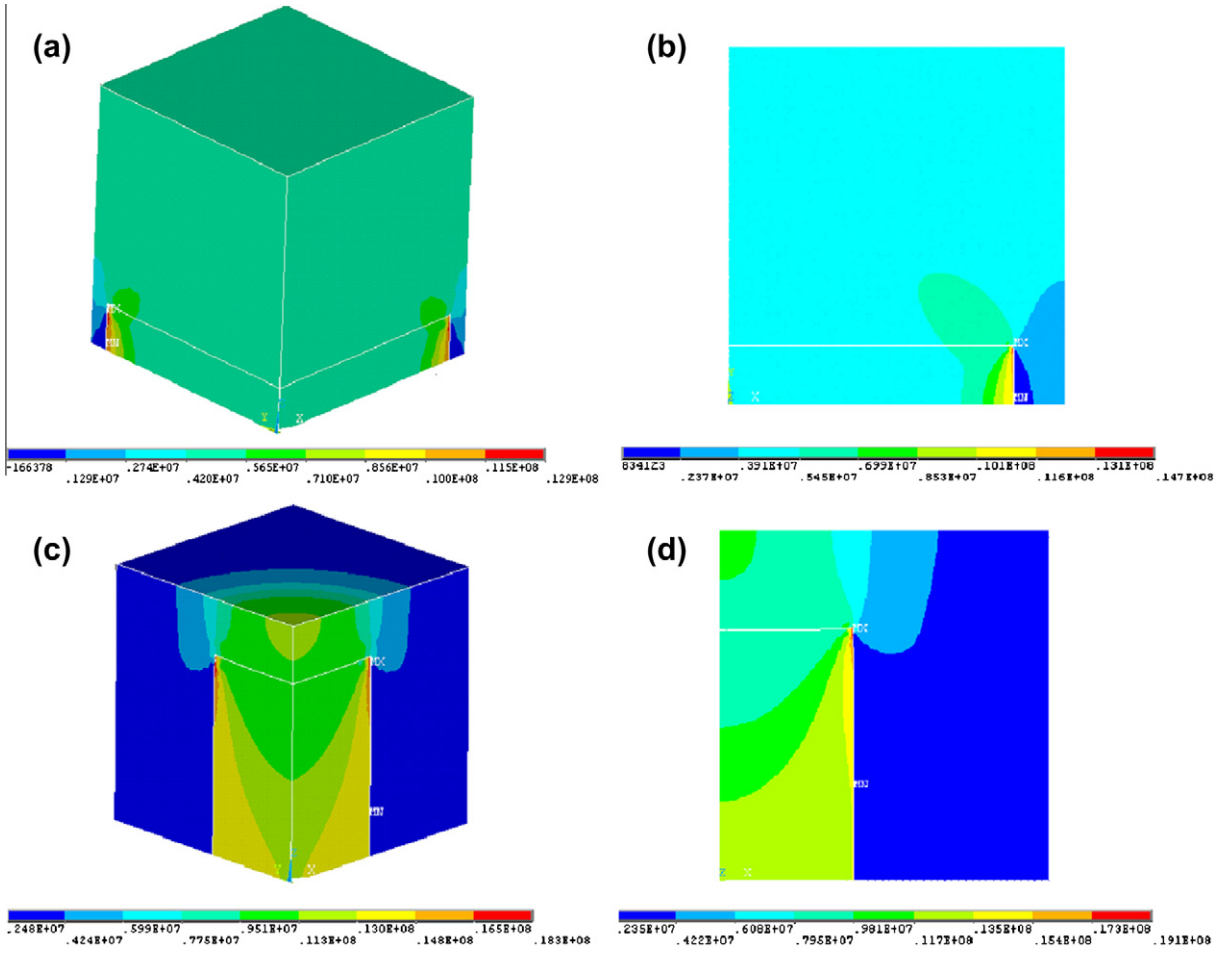

Fig. 6. Maximum axial stress distribution for the RVEs under uniaxial load for the MMC reinforced with particles: (a) aspect ratio of 0.2 using a 3-D RVE, (b) aspect ratio of 0.2 using an axisymmetric 2-D model, (c) aspect ratio of 1.8 using a 3-D RVE, and (d) aspect ratio of 1.8 using an axisymmetric 2-D model.

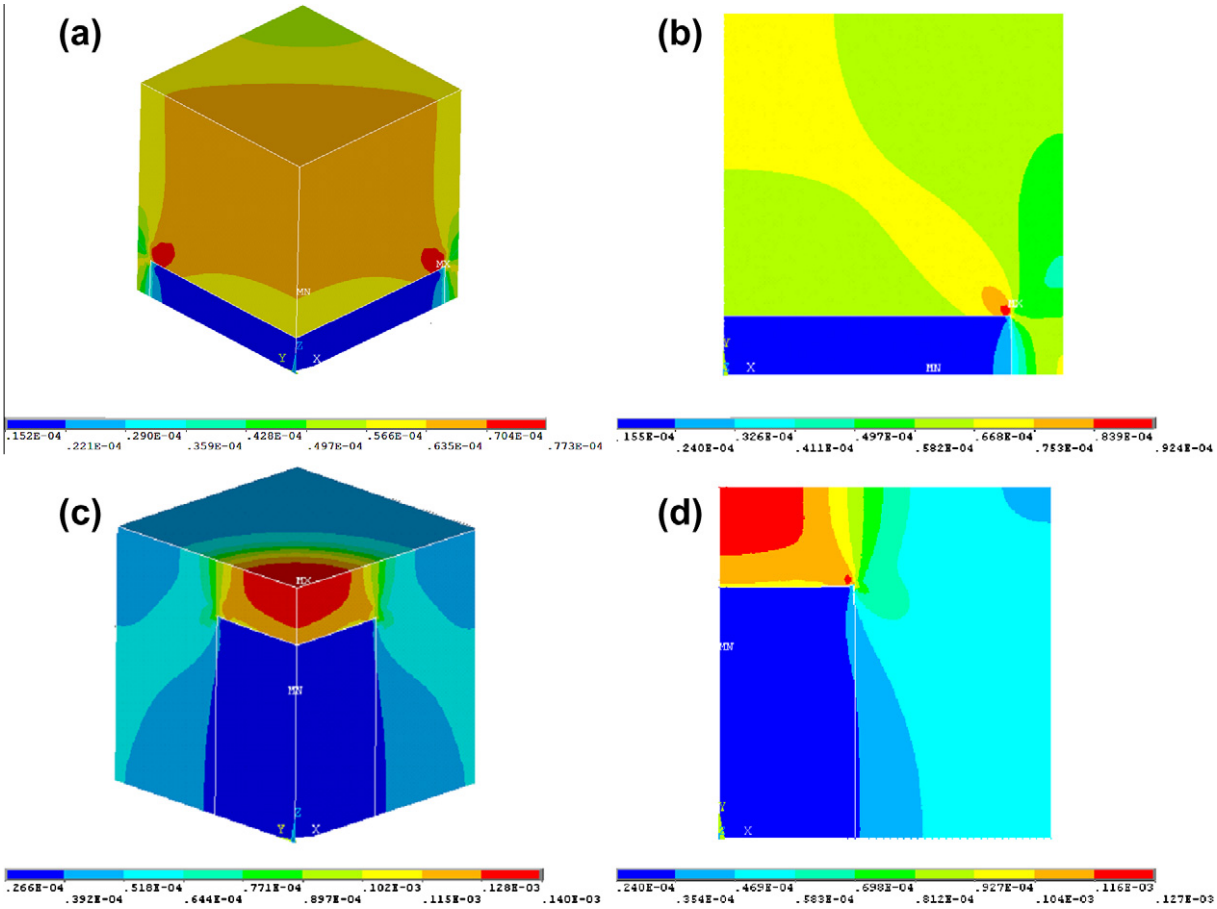

Fig. 7. Maximum axial strain distribution for the RVEs under uniaxial load for the MMC reinforced with particles: (a) aspect ratio of 0.2 using a 3-D RVE, (b) aspect ratio of 0.2 using an axisymmetric 2-D model, (c) aspect ratio of 1.8 using a 3-D RVE, and (d) aspect ratio of 1.8 using an axisymmetric 2-D model.

D model allowed observing points out of reach for the axisymmetric model (points at the corner).

In order to analyze the differences for the cylindrical (2-D model) and the cubic (3-D model) RVEs, the dimensions of the unit cells were studied, emphasizing in the relationship between the heights and transversal areas for the particle-RVE systems. As already mentioned, the particle-RVE volume relationship was constant for both, cylindrical and cubic RVEs, where $V_{particle}/V_{RVE} = 0.12$. As expected, the relationships between the heights of the RVEs and the particles ($H_{RVE}/h_{particle}$) changed. The relationships between the transversal areas ($A_{RVE}/a_{particle}$) also changed. As can be observed in Fig. 8a, the relationship $H_{RVE}/h_{particle}$ decreased with the aspect ratio, being 7.78% higher for the cylinder than for the cube for all the aspect ratios. In addition, the relationship $A_{RVE}/a_{particle}$ increased with the aspect ratio, as shown in Fig. 8b, being 7.65% higher for the square (transversal area of the cube) than for the circle (transversal area of the cylinder) for all the aspect ratios.

These results could help to explain the differences between the estimated values for 2-D and 3-D models for different aspect ratios. First, the Young's Moduli estimation, obtained from axial deformation i.e. higher $H_{RVE}/h_{particle}$ relationship for the cylinder would leads to a higher deformation for the 2-D model, while a higher $A_{RVE}/a_{particle}$ relationship for the square would leads to a higher deformation for the 3-D model. The $H_{RVE}/h_{particle}$ difference (7.78%) is slightly higher than the $A_{RVE}/a_{particle}$ difference (7.65%), results that suggest a higher Young's modulus for the 3-D model. This difference has not effect at low aspect ratios, where the reinforcement effect is low, and Young's Moduli were almost the same for both RVEs (Fig. 3a). Nevertheless, for high aspect ratios the MMC is more susceptible to small changes in the RVE shape, and the Young's modulus was higher for the 3-D model, as predicted by the geometrical analysis.

Finally, these facts could also explain the stress and strain behavior observed in Fig. 5a and b, respectively. The lowest $A_{RVE}/a_{particle}$ relationship for the circle provokes the highest maxima axial stress and strain for the cylindrical RVE at low aspect ratios. At higher aspect ratios the $H_{RVE}/h_{particle}$ effect is more important and the maxima values are closer. Even maxima strains are located in the cubic RVE for aspect ratios higher than 1.0.

4. Conclusions

In this work, a three-dimensional model was presented in order to study the behavior of a particulate reinforced MMC with different aspect ratios, subjected to an axial load. A 2-D axisymmetric model was also used for comparative purposes. The elastic moduli estimated using both 2-D and 3-D FEA models are close to those predicted by the Halpin–Tsai model. The results of the calculated Young's modulus using the proposed 3-D FEA model was in better agreement with the experimental results than those obtained by the Halpin–Tsai model and the 2-D FEA model. Qualitative differences were not obtained when comparing 2-D and 3-D models: deformation, stress and strain distributions showed an excellent agreement. Nevertheless, quantitative differences were observed for the estimations obtained using these models: Young's modulus was higher for the 3-D model, mainly for higher aspect ratios; maxima stresses and strains were higher for the 2-D model at low aspect ratios, while at higher aspect ratios the maxima corre-

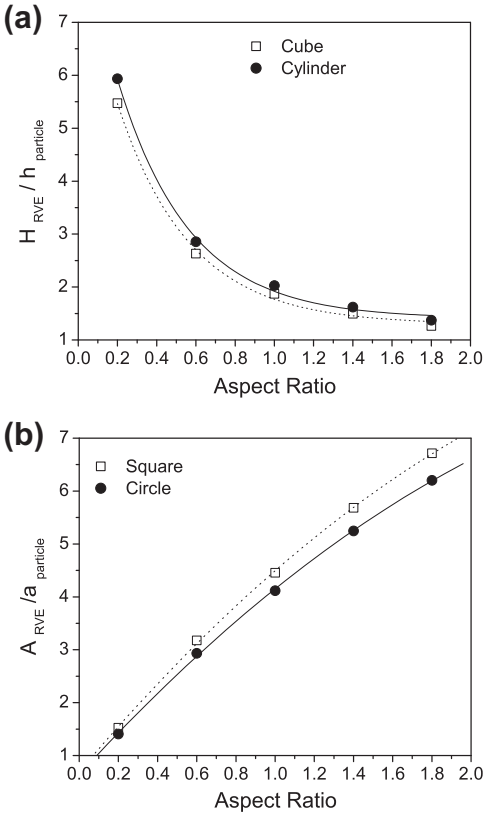

Fig. 8. Geometrical characteristics of the 2-D and 3-D RVEs for different aspect ratios: (a) $H_{RVE}/h_{particle}$ relationship, and (b) $A_{RVE}/a_{particle}$ relationship.

spond to the 3-D model estimations. This behavior could be explained due to geometrical differences between selected unit cell, mainly in transversal area and height. Besides, the 3-D model allowed observing points out of reach for the axisymmetric model. The results suggest that the 3-D model with one-eight part of the unit-cell as the representative volumetric element can be successfully used to model the mechanical behavior of a MMC.

Acknowledgements

This research was supported by SENER-CONACYT and Secretaria de Educacion Publica with Grants number "151496" and "PROMEP/103.5/11/66", respectively. A. Tejeda-Cruz, E.A. Caballero-Rodríguez, G.A. Lara-Rodríguez, J.J. Camacho, J. Morales-Rosales, R. Reyes-Ortiz, C. Flores-Morales, O. Novelo-Peralta, C. González, E. Sanchéz, J. Morales and M.J. Arellano are also acknowledged for their technical support.

References

[1] Engineering Materials Handbook. Volume 1: Composites, third ed., ASM International, Metals Park, Ohio, 1989.
[2] S. Suresh, A. Mortensen, A. Needleman (Eds.), Fundamentals of Metal Matrix Composites, Butterworth/Heinemann, Boston, 1993.
[3] R.K. Everett, R.J. Arsenault (Eds.), Metal Matrix Composites: Processing and Interface, Academic Press, New York, 1991.
[4] S. Wilson, A. Ball, Tribology of Composite Materials, ASM International, Metals Park, Ohio, 1990.
[5] R. Hill, J. Mech. Phys. Solid 13 (1965) 213–222.
[6] Z. Hashin, B.W. Rosen, J. Appl. Mech. 31 (1964) 223–232.
[7] J.D. Eshelby, Proc. R. Soc. Lond. A241 (1957) 376–396.
[8] I. Ahmadi, M.M. Aghdam, J. Mech. Eng. Sci. 224 (2010) 1567.
[9] M.M. Aghdam, D.J. Smith, M.J. Pavier, J. Mech. Phys. Solid 48 (2000) 499–528.
[10] M.M. Aghdam, M.J. Pavier, D.J. Smith, Int. J. Solid Struct. 38 (2001) 3905–3925.
[11] C.T. Sun, R.S. Vaidya, Compos. Sci. Technol. 56 (1996) 171–179.
[12] J.C. Halpin, S.W. Tsai, Environmental factors in composite materials design, Air Force Mater. Lab. (1967) TR 67-423.
[13] V.V. Ganesh, N. Chawla, Mater. Sci. Eng. A 391 (2005) 342–353.
[14] R.D. Cook, D.S. Malkus, M.E. Plesha, Concepts and Applications of Finite Element Analysis, third ed., John Wiley & Sons, New York, 1989.
[15] S. Kari, H. Berger, U. Gabbert, Comp. Mater. Sci. 39 (2007) 198–204.
[16] N. Srikanth, C. Voon Lim, M. Gupta, J. Mater. Sci. 35 (2000) 4661–4666.
[17] Y.J. Liu, X.L. Chen, Elect. J. Bound. Elem. 1 (2003) 316–335.
[18] A. McLean, H. Soda, Q. Xia, A.K. Pramanick, A. Ohno, G. Motoyasu, T. Shimizu, S.A. Gedeon, T. North, Compos. Part A Appl. Sci. 28 (1997) 153–162.
[19] Metals Handbook. Volume 2. Properties and Selection: Nonferrous Alloys and Special-Purpose Materials, 10th ed., ASM International, Metals Park, Ohio, 1990.
[20] S.P. Gurrum, J. Zhao, D.R. Edwards, J. Mater. Sci. 46 (2011) 104.
[21] Y.L. Shen, M. Finot, A. Needleman, S. Suresh, Acta Metall. Mater. 43 (1995) 1701.
[22] H.K. Jung, Y.M. Cheong, H.J. Ryu, S.H. Hong, Scripta Mater. 41 (1999) 1261–1267.
[23] J.C. Lee, K.N. Subramanian, J. Mater. Sci. 29 (1994) 4901.
[24] I.M. Robinson, J.M. Robinson, J. Mater. Sci. 29 (1994) 4663–4677.
[25] S.H. Chen, T.C. Wang, Acta Mech. 157 (2002) 113–127.
[26] N. Chawla, K.K. Chawla, J. Mater. Sci. 41 (2006) 913–925.
[27] X. Xia, H.J. Mcquee, H. Zhu, Appl. Compos. Mater. 9 (2002) 17–31.